

Coordinated Scheduling of Residential Distributed Energy Resources to Optimize Smart Home Energy Services

Michael Angelo A. Pedrasa, *Student Member, IEEE*, Ted D. Spooner, and Iain F. MacGill

Abstract—We describe algorithmic enhancements to a decision-support tool that residential consumers can utilize to optimize their acquisition of electrical energy services. The decision-support tool optimizes energy services provision by enabling end users to first assign values to desired energy services, and then scheduling their available distributed energy resources (DER) to maximize net benefits. We chose particle swarm optimization (PSO) to solve the corresponding optimization problem because of its straightforward implementation and demonstrated ability to generate near-optimal schedules within manageable computation times. We improve the basic formulation of cooperative PSO by introducing stochastic repulsion among the particles. The improved DER schedules are then used to investigate the potential consumer value added by coordinated DER scheduling. This is computed by comparing the end-user costs obtained with the enhanced algorithm simultaneously scheduling all DER, against the costs when each DER schedule is solved separately. This comparison enables the end users to determine whether their mix of energy service needs, available DER and electricity tariff arrangements might warrant solving the more complex coordinated scheduling problem, or instead, decomposing the problem into multiple simpler optimizations.

Index Terms—Coevolutionary PSO, distributed energy resources, energy management, energy services, home automation, optimization methods, repulsive PSO, value of coordination.

I. INTRODUCTION

SMART HOMES are residential buildings equipped with devices that coordinate with each other using communication channels in order to achieve a common set of goals that benefit the end users [1], [2]. Examples of goals are the management of energy consumption, provision of comfort and security, and provision of home-based health care and assistance to elderly or disabled users.

Several hardware and software platforms have been proposed to realize a smart home from the perspective of energy service provision and energy conservation and management [3]–[7]. These systems give the end users the opportunity to monitor and to remotely control key equipment within their homes and also

implement rule-based decision-making with respect to their operations. Some systems also propose the incorporation of location-management frameworks that could learn and predict occupant location and routes [8] or learn and recognize occupant activities [9].

In this paper, we describe enhancements to an energy service decision-support tool previously described in [10]. The decision-support tool aims to aid households in making more intelligent decisions when operating their major home appliances, and it can operate on top of the enabling-technologies listed above. The decision-support tool is based on maximizing the net benefits gained by the end users when they utilize energy services.

The decision-support tool is based around an energy service model that enables end users to place a received benefit on key energy services. A scheduling algorithm attempts to maximize the net benefits for the end user—that is, the total energy service benefits minus the costs of energy provision. The costs may often vary with time (e.g., time-of-use tariffs) and have other components (e.g., peak demand charges).

In this paper, we also describe a smart home case study which is an extended version of the case study presented in [10]. In the case study, the scheduler determines the operation schedule of four distributed energy resources (DER) that maximize the net benefits of the end user. The resulting optimization problem is complex, and beyond the PSO solver described in [10]. This work used a coevolutionary version of particle swarm optimization (CPSO) to generate the schedules. PSO was because of its ease in implementation and because it proved able to generate feasible solutions within manageable computation times.

The more complex case study in this paper, however, revealed limitations to this algorithm. In this paper, we present some variations of CPSO that have stochastic repulsion among the particles (CPSO-R) and determine which of these variations can generate the best solutions to the case study at hand.

Using the enhanced PSO solver, we quantify the value added by coordination among the DER. We determine the value of coordination by scheduling each DER independent of the others, and compare the costs incurred by the end users to that when the DER are cooperating. This exercise will give the end user insights on those circumstances (e.g., tariff arrangements) when coordination among DER is important, and when it is not. It also identifies the circumstances when the high-dimension optimization problem may be decomposed into several simpler optimization problems.

The rest of the paper is summarized as follows: the decision-support tool and the case study are discussed in Section II, the

Manuscript received February 09, 2010; revised May 02, 2010; accepted June 07, 2010. Date of publication July 26, 2010; date of current version August 20, 2010. The work of M. A. Pedrasa was supported by the University of the Philippines (DSF) and the Philippines DOST-SEI Engineering Research and Development for Technology Program. Paper no. TSG-00023-2010.

The authors are with the Centre for Energy and Environmental Markets and School of Electrical Engineering and Telecommunications, University of New South Wales, Sydney NSW 2052, Australia (e-mail: m.pedrasa@student.unsw.edu.au).

Digital Object Identifier 10.1109/TSG.2010.2053053

PSO solution to the corresponding mathematical optimization problem is presented in Section III, the value of coordination among the DER is presented in Section IV, and our conclusions are summarized in Section V.

II. SCHEDULING OF DER FOR OPTIMIZED RESIDENTIAL ENERGY SERVICE ACQUISITION

A. Energy Services and Distributed Energy Resources

Energy services are energy forms and processes from which end users ultimately derive and realize the value of energy carriers like electricity and gas [11]. Common forms of residential energy services are space conditioning (cooling and heating), illumination, food storage and preparation, water heating, and entertainment. By suitably scheduling the operation of controllable DER, residential end users can potentially improve the acquisition of their energy services. DER are fine-grained equipment and practices usually colocated or near the energy service end user. Common examples of DER are distributed generation, energy storage and controllable end-use loads.

Several methods that control the operation of DER to optimize energy services acquisition are described in the literature. These approaches include appliance start-time enumeration [12], agent-based appliance control systems enhanced with tabu search or genetic algorithms [13], [14], and model predictive control [15]. Our decision-support tool differ from these approaches by recognizing that end users put different levels of benefit to different services at different hours of the day, and by considering these benefits as we optimize the DER operation schedules.

B. Decision-Support Tool

We presented in [10] a decision-support tool that end-users can use to optimize their acquisition of energy services. The decision-support tool is composed of an energy service model and a DER scheduling algorithm. The energy service model represents the demand for and the benefit end users derive from energy services. The demand for an energy service is described by specifying the hourly variation of a variable directly related to the service, or the hourly variation of the demand for the energy that realizes the service. As an example, the demand for hot water may be specified as the hourly volume of hot water consumption, or the hourly consumption of the heat energy content of the water. In this example, the heat content of water is said to be the “energy equivalent” of the hot water service. The energy service model represents the benefit end users derive from an energy service by assigning a monetary benefit to each unit of “energy equivalent.”

The scheduling algorithm determines the operation schedules of controllable DER that maximize the net benefit to the end user. The net benefit is equal to the benefit derived from the energy services less the cost of energy consumption. The scheduling is a mathematical optimization problem described by the maximization of the following fitness function:

$$\sum_{t=1}^T \sum_{i=1}^S [\lambda_{ES,i}(t) \cdot U_{ES,i}(t, \mathbf{x})] - Cost \quad (1)$$

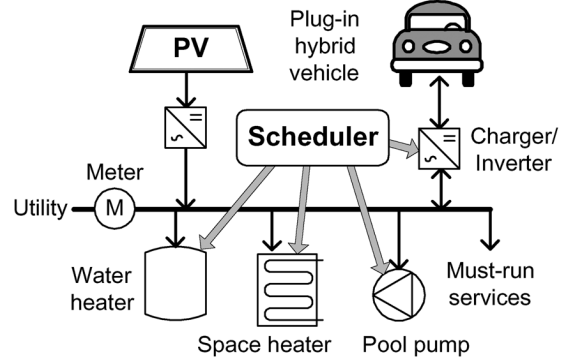


Fig. 1. Extended version of the smart home case study in [10].

$\lambda_{ES,i}$ is the monetary benefit assigned to each unit of “energy equivalent” of the i^{th} service, $U_{ES,i}$ is the demand for the “energy equivalent” of the i^{th} service, and \mathbf{x} is the DER operation schedule. S is the number of services and T is the simulation horizon. The double summation term adds up the benefit derived from all services over the entire simulation period and subtracted from it is the cost ($Cost$) of electricity consumption. $Cost$ includes the energy charges, and credits for energy export and peak demand charges if applicable.

C. Case Study

The case study we presented in [10] involves the optimization of energy service provision in a smart home. We extended the case study by changing the battery storage into a plug-in hybrid vehicle and by using a storage water heater to provide the hot water service. Fig. 1 describes the case study. The DER and their characteristics are listed below and the operation of the first four are determined by the scheduler.

- 1) Plug-in hybrid vehicle (PHEV). 5.9 kWh capacity, 3.0 kW maximum charging/discharging rate, 90% charging/discharging efficiency, may be discharged down to 30% of capacity, 0.1% coulomb loss per hour.
- 2) Space heater. Maximum heating power is 1.8 kW.
- 3) Storage water heater. Storage capacity is 80 liters and the heating element is rated 1.2 kW.
- 4) Pool pump. Rated 1.1 kW. Should run at most 6 hours.
- 5) PV system. Peak output = 2.0 kW.

The scheduler determines the hourly charging or discharging rate of the PHEV battery, the hourly heating power of the space heater, the hours when the water heater will be switched on, and the hours when the pool pump is run.

All energy services aside from PHEV charging, space and water heating, and pool pumping are lumped together into an aggregate must-run energy service. The must-run service includes food storage and preparation, illumination, entertainment, etc. The demand for the services are shown in Fig. 2.

The function of the scheduler is to determine the DER operation schedules that maximize the net benefits. Based on (1), the corresponding optimization problem is to find the DER operation schedules $\mathbf{x} = [\mathbf{x}_{car} \ \mathbf{x}_{heat} \ \mathbf{x}_{water} \ \mathbf{x}_{pool}]$ that maximizes

$$\begin{aligned} & \sum_{t=1}^T (\lambda_{ES,must-run}(t) \cdot U_{ES,must-run}(t) \\ & + \lambda_{ES,car}(t) \cdot U_{ES,car}(t, \mathbf{x}_{car}) \\ & + \lambda_{ES,heat}(t) \cdot U_{ES,heat}(t, \mathbf{x}_{heat}) \end{aligned}$$

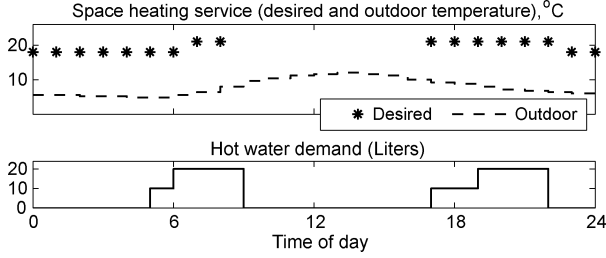
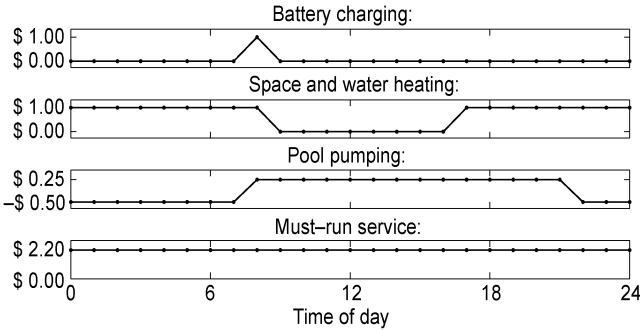


Fig. 2. Hourly demand for the energy services.

TABLE I
ELECTRICITY TARIFF STRUCTURES

Tariff, $\lambda_e(t)$	Rate
Time of Use (ToU) (\$/kWh) [16]	
Peak: 2 – 8 PM	0.3564
Shoulder: 7 AM – 2 PM, 8 – 10 PM	0.1408
Off-peak: 10 PM – 7 AM	0.0814
Critical peak price (CPP), 5 – 8 PM (\$/kWh) [17]	2.000
Capacity (or peak demand) charge 2 – 8 PM only (\$/kW) [18]	0.128186

Fig. 3. Perceived benefit derived from each kWh of “energy equivalent,” $\lambda_{ES}(t)$.

$$\begin{aligned}
 & + \lambda_{ES,water}(t) \cdot U_{ES,water}(t, \mathbf{x}_{water}) \\
 & + \lambda_{ES,pool}(t) \cdot U_{ES,pool}(t, \mathbf{x}_{pool}) \\
 & - \lambda_e(t) \cdot P_e(t, \mathbf{x}).
 \end{aligned} \quad (2)$$

The first five products are the benefits derived from the services, while the last product is the cost of electricity consumption. T is the simulation horizon, λ_e is the cost of electricity or feed-in rate, and P_e is the hourly energy consumption

$$P_e = P_{e,must-run} + P_{e,car} + P_{e,heat} + P_{e,water} + P_{e,pool} - P_{PV}. \quad (3)$$

The electricity rates are shown in Table I.

The benefit derived by the end users to each kWh of “energy equivalent” of the services are shown in Fig. 3. The monetary values are based on the end users’ perception on the importance of these respective services. The hourly values depicted in the figure represent the case that: a) the PHEV should be fully charged at 8 AM but the residents do not care about the state of charge at any other hour; b) the end users do not care about the temperature inside the house and if hot water is available between 8 AM and 5 PM (when they are at work) but puts a high value to these services when they are home; c) the pool pumps should run anytime between 8 AM and 10 PM and should not run beyond those hours due to noise considerations (hence the

negative benefit values); and d) the must-run service should be delivered regardless of the cost of electricity.

The energy service model also relates the “energy equivalent” of the services to the electric energy consumption of the end-use equipment, or DER, that provides the service. The “energy equivalent” of the space and water heating services are the thermal energy content of indoor air and water, while the “energy equivalent” of the PHEV charging service is the energy stored in the batteries. In [19], we used physically-based models to relate the “energy equivalent” of these services to the hourly energy consumption. For the must-run and pool pumping services, the actual energy consumption is taken as the “energy equivalent.” For immediate reference, the models for the space heating and hot water services are described in Appendix A.

The total cost incurred by the end user is equal to the cost of electricity consumption plus the cost of the services that were not delivered. We propose this formula for cost computation because it reflects the benefits not gained by the end user from the services that were not provided. The costs of the undelivered services are equal to the benefits that were not gained. For the case study, the cost of the undelivered services are determined from:

- 1) the amount of energy required to fully charge the PHEV battery if it is not fully charged;
- 2) the difference of the actual room temperature from the desired temperature if it is beyond the comfortable range;
- 3) the amount of hot water that is not delivered;
- 4) the number of hours that the pool pump did not run if it did not run for 6 h.

III. DER SCHEDULING USING PARTICLE SWARM OPTIMIZATION

A. Particle Swarm Optimization and Variations

Particle swarm optimization is a heuristic population-based search technique that locates the solution to an optimization problem by allowing candidate solutions (or particles) to fly around the solution space, with their trajectories affected by the best performing candidate solution (Gb) and the best location they have visited (Pb) [20]. The movement of the particles in canonical PSO are described by the following equations:

$$v_{i,k}^{t+1} = \omega v_{i,k}^t + c_1 r() (p_{Gb,i}^t - p_{i,k}^t) + c_2 r() (p_{Pb,i}^t - p_{i,k}^t) \quad (4)$$

$$p_{i,k}^{t+1} = p_{i,k}^t + v_{i,k}^{t+1} \quad (5)$$

where $V_k(v_{1,k}, \dots, v_{n,k})$ and $P_k(p_{1,k}, \dots, p_{n,k})$ are the velocity and position of the k^{th} particle. The constants ω , c_1 , and c_2 are the weights of the particles’ momentum, and pull of the personal and global best positions, and $r()$ is a uniform random number within [0,1].

The particle positions and velocities are randomly initialized. Afterwards, they move around the solution space guided by (4) and (5). The fitness of all particles are evaluated and the global and personal best positions are updated if needed. The global best at the end of the simulation is taken as the solution to the problem.

Binary PSO may be used if the optimization involves binary-valued or binary-coded decisions [21]. In binary PSO, the

speed of a particle coordinate is mapped to a probability using a sigmoid function, and the resulting probability determines whether the coordinate would take a value of 1 or 0. The speed is also computed using (2), but it is restricted to be within the range $[-V_{max}, V_{max}]$.

Cooperative coevolution may be used with PSO if the optimization problem involves a large number of decision variables [22]. This approach uses a divide-and-conquer approach: the vector to be optimized is divided into several components and a swarm is used to optimize each component. The fitness of a particle belonging to one of the swarm is determined by concatenating it with the current global best particles of the other swarms.

In [23], premature convergence of the particles is avoided by changing the direction of the attraction of the global and personal best positions in (4) according to the diversity of the particles. A method for measuring the diversity of the particles is proposed and it involves the computation of distances of particles from the centroid of the swarm. Therefore, speed is computed by

$$v_{i,k}^{t+1} = \omega v_{i,k}^t - c_1 r() (p_{Gb,i}^t - p_{i,k}^t) - c_2 r() (p_{Pb,i}^t - p_{i,k}^t) \quad (6)$$

if the particles come too close together as indicated by the diversity measure. [24] introduced another variation where a third expression (7) for particle speed is used if the diversity is midway from being too crowded and being too dispersed

$$v_{i,k}^{t+1} = \omega v_{i,k}^t - c_1 r() (p_{Gb,i}^t - p_{i,k}^t) + c_2 r() (p_{Pb,i}^t - p_{i,k}^t). \quad (7)$$

We chose PSO to solve the DER schedules in the case study described in Section II-C because of several reasons, most important of which are the ease in implementation and its ability to generate near-optimal solutions within manageable timeframes. We only need to encode simple behaviors to an ample amount of particles and the interaction among the particles enable the swarm to achieve complex behaviors. In this case, PSO can find feasible solutions for a complex optimization problem. We also chose PSO because of its ability to handle complex models. In particular to the problem we are trying to solve, it can handle: a) the separation between the value of and the demand for energy services with respect to time; b) complex energy supply models, i.e., different electricity tariff arrangements like ToU, feed-in tariff and peak demand charges; and c) complex DER and energy service models, e.g., relationship between indoor temperature to space heating power and outdoor temperature, and relationship between discharged hot water to the state of the water heater (ON or OFF). Finally, coevolution enables PSO to find near-optimal solutions for high-dimensional problems.

B. Solving the Case Study Using Coevolutionary PSO

We used coevolutionary PSO to solve the DER schedules in the case study described in Section II-C [19]. Canonical PSO is used to optimize DER schedules with real-value coordinates, while binary PSO is used to optimize the schedules with binary coordinates. To improve the performance of the coevolutionary PSO solver, we adopted the repulsion among the particles as described in [23], [24].

For the CPSO, we used ten swarms to determine the operation schedules of the four DER: three swarms optimize the charging of the PHEV, three swarms optimize the space heater power, three swarms optimize the water heater schedule and one swarm optimizes the pool pumping schedule. The PHEV charging, and the space and water heater schedules are divided into three 8-coordinate vectors and a swarm is used to optimize each 8-h vector. Canonical PSO is used to determine the hourly charging or discharging rates of the battery, the heating power of the space heater, and the starting times of the three 2-h pool pumping periods. Binary PSO is used to determine whether the water heater is to be connected to the supply or not. In each iteration, the order at which the four DER schedules are evolved is chosen randomly but the 3 swarms assigned to the PHEV and heaters are evolved in chronological order.

The swarms guided by canonical PSO have 50 particles while the swarms guided by binary PSO have 20 particles. The parameters used for canonical PSO are $\omega = 0.7298$ and $c_1 = c_2 = 1.4962$, and for binary PSO, $\omega = 1.0$, $c_1 = c_2 = 7.5$, and $V_{max} = 5.0$. These sets of parameters were effective in generating near-optimal solutions in [25] (for canonical PSO) and [26] (for binary PSO). The simulation has 120 iterations. The constraints are handled using a repair algorithm [27], that is, the coordinates that violate the constraints are corrected at each iteration.

One simulation result is shown in Fig. 4. In this case, the house is under time-of-use tariff and there is no credit for any exported energy. Critical peak pricing is also active from 5–8 PM. The residents leave the PHEV at home so it is used as a storage DER. The figure shows the indoor temperature, the state of charge of the PHEV battery, the hourly energy consumptions of the space and water heaters and the pool pump, and the hourly total energy consumption. In this case, the PHEV is fully charged at 8 AM, all required hot water is provided, and the pool pump is run for 6 h. The indoor temperature is below the comfortable range at 8 PM so at this hour, the space heating service is not delivered. The energy stored in the PHEV battery is discharged, and that energy is partly consumed by the space heater and the rest by the must-run service. The four DER also coordinate their operation so that no PV energy is exported, and to minimize grid import during the peak and CPP periods. The total cost incurred by the end user is \$7.07 while the cost of electricity consumption is \$6.08. Since all services except the space heating service are fully delivered, the difference is equal to the benefit not gained due to the 1 h that the indoor temperature is beyond the comfortable range.

C. Coevolutionary PSO With Stochastic Repulsion Among Particles

We observed in our simulations in [19] that the solutions converged prematurely so there was a need to improve the performance of CPSO. To delay convergence and to better search the solution space, we incorporated repulsive forces among the particles similar to that of [23] and [24], but did away with the consideration of diversity which tends to be computationally expensive. Instead, a coordinate of a particle may move away from the global and personal best positions at any iteration and this behavior is conditional to a certain probability function. In

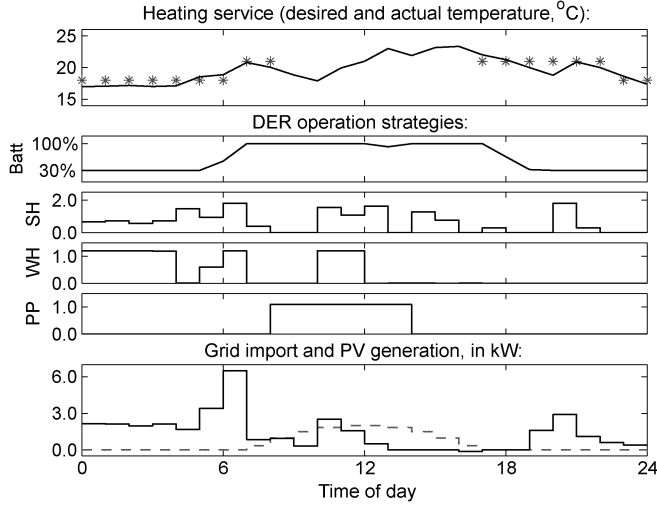


Fig. 4. DER schedules for the case where there is no credit for any energy export and CPP is active from 5 to 8 PM. Shown are the state of charge of the PHEV battery (Batt), and the hourly energy consumption of the space heater (SH), water heater (WH), and pool pump (PP). Also shown are the hourly grid energy import and PV energy output (broken line).

our simulations, the probability that a coordinate moves away from the global and personal bests is 50% on iteration 1 and this probability linearly decrease to zero until iteration 80. From iterations 81 to 120, all particles are guided by (4) and (5). We investigated the four variations of CPSO-R described by the speed computation in (8) and the influence of the global and personal best positions outlined in Table II

$$v_{i,k}^{t+1} = S_M \omega v_{i,k}^t + S_{Gc1} r() (p_{Gb,i}^t - p_{i,k}^t) + S_{Pc2} r() (p_{Pb,i}^t - p_{i,k}^t). \quad (8)$$

We chose a fixed number of evolutions so that we could observe the convergence of all CPSO-R variants, and we could compare the improvement of the global best fitness for all variants at the same number of evolutions.

CPSO-R1 is adopted from [24]. If a coordinate is repulsed, it tends to move away from the global best but there is equal chance that it will move closer or away from the personal best. CPSO-R2 is adopted from [23]; the coordinate tends to move away from the global and personal best positions when it is repulsed.

CPSO-R3 and CPSO-R4 are our variations. When a coordinate is repulsed in CPSO-R3, it traverses the path opposite the direction computed by CPSO. In CPSO-R4, the coordinate is repulsed both by the global and personal best positions and completely loses the momentum component.

We compared the performance of the CPSO-R variants to that of CPSO using the case study. We investigated the cases where the smart home is under the following tariff structures:

- 1) Tariff A: ToU energy with ToU feed-in rates;
- 2) Tariff B: ToU energy with no feed-in compensation;
- 3) Tariff C: ToU energy with ToU feed-in rates and peak demand charges.

We also considered two possible states each for:

- a) solar insolation (entire day is sunny or cloudy);

- b) availability of the PHEV as storage device from 8 AM to 5 PM (if the residents use the car or not when they go to work);
- c) demand for must-run and hot water services (normal demand or low demand);
- d) state of critical peak pricing (CPP, active or not).

Therefore, there are 16 possible scenarios to be investigated for each tariff structure.

The simulation was done using Matlab R2008b on Windows XP, running on a 2.0-GHz dual CPU. Each scenario is simulated 20 times and the best schedule is chosen. We repeated the simulation several times to determine the consistency of each variant in finding good solutions. Furthermore, we recognize that PSO can only generate near-optimal solutions, hence, repetition allows it to discover better solutions. Each simulation is around 32 s long, thus 20 repetitions last around 10.5 min.

The simulation results in Table III shows the average increase of fitness values and average decrease in costs of the best schedules of the CPSO-R results with respect to the CPSO result, and the standard deviation of fitness values averaged over all scenarios and all tariff structures. The cost is computed by adding the cost of energy to the cost (or loss of benefit) of undelivered services. The improvement of the global best fitness for all variants in one of the scenarios are shown in Fig. 5.

The table shows that CPSO-R3 is best among the four variants in solving the current optimization problem since it produced the largest average improvement in fitness and costs with respect to CPSO. Furthermore, it is most consistent since the fitness of the 20 schedules are closer to each other when compared to the other variations. The improvements were achieved with no additional computation time.

Fig. 5 reveals that CPSO-R3 does not converge prematurely like CPSO, but the other variants take a little longer to converge. In CPSO-R3, the momentum component either pushes the particle coordinate away or closer to the former personal and global best positions. That is, if the coordinate moved away from these positions in the previous iteration, then the changing sign of the momentum particle in the current iteration would push the coordinates to the former global and personal best positions. Therefore, CPSO-R3 adds the most amount of randomness to the particle movements at the earlier stages of the simulation among the four variations, and this could have caused the better performance. We acknowledge that more intensive comparisons using benchmark objective functions and trajectory analysis should be done before stronger conclusions can be made. There is also a need to compare which of the two methods of incorporating repulsion (stochastic or diversity-driven) is better.

IV. VALUE OF COORDINATION AMONG DER

In most cases, optimal acquisition of energy services can only be achieved if the DER cooperate with each other. In this section, we use best version of CPSO-R to determine the value added by the coordination among the DER to the consumer's net benefit. This exercise enables the end users to identify the scenarios in which the DER should work together and the scenarios in which the DER can be independently scheduled. It also identifies the situations where the complex scheduling problem may be decomposed into several smaller problems.

TABLE II
VARIATIONS OF CPSO WITH STOCHASTIC REPULSION AMONG PARTICLES

Variant Name	S_M	S_G	S_P
CPSO (canonical co-evolutionary PSO)	+1	+1	+1
CPSO-R1	+1	-1	± 1
CPSO-R2	+1	-1	-1
CPSO-R3	-1	-1	-1
CPSO-R4	0	-1	-1

TABLE III
COMPARISON OF RESULTS BETWEEN CPSO AND CPSO-R

	Best schedules of 16 scenarios		Average standard deviation of fitness over all scenarios
	Average fitness increase*, %	Average cost decrease*, %	
Tariff A: ToU energy + ToU feed-in:			
CPSO			0.263
CPSO-R1	0.083	0.474	0.164
CPSO-R2	0.061	0.078	0.196
CPSO-R3	0.287	1.950	0.122
CPSO-R4	0.123	0.789	0.149
Tariff B: ToU energy + no feed-in			
CPSO			0.209
CPSO-R1	0.082	0.514	0.139
CPSO-R2	0.084	0.477	0.166
CPSO-R3	0.138	0.683	0.065
CPSO-R4	0.090	0.483	0.115
Tariff C: ToU energy + ToU feed-in + capacity charges			
CPSO			0.240
CPSO-R1	0.108	0.551	0.142
CPSO-R2	0.081	0.448	0.163
CPSO-R3	0.178	1.093	0.086
CPSO-R4	0.133	0.800	0.115

* With respect to CPSO

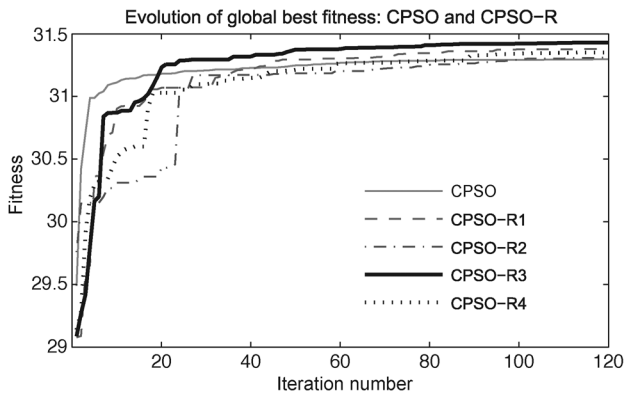


Fig. 5. Improvement of the fitness of the global best for all variants of CPSO-R in one of the scenarios.

We determine the value of coordination among the DER by scheduling each DER independent of the others and compare the results to that when they are working together to maximize net benefits. An independent DER schedule is created by assuming that the service that DER is providing and the must-run services are the only ones to be acquired. We still used (2), but only include the terms related to the DER being scheduled. To

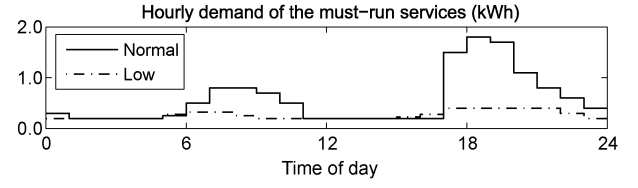


Fig. 6. Expected electricity demand of the must-run services.

TABLE IV
SUMMARY OF SCENARIO CODES

Condition	Value of X	
	1	0
S: Solar insolation	Sunny	Cloudy
D: Demand for must-run and hot water services	Normal	Low*
B: PHEV available from 8 AM to 5 PM	Yes	No
C: Critical Peak Pricing	Yes	No

* See Fig. 6 for must-run service. Hot water demand is 25% of normal

illustrate, the PHEV charging schedule is solved by finding \mathbf{x}_{car} that maximizes

$$\sum_{t=1}^T (\lambda_{ES,must-run}(t) \cdot U_{ES,must-run}(t) + \lambda_{ES,car}(t) \cdot U_{ES,car}(t, \mathbf{x}_{car}) - \lambda_e(t) \cdot P_e(t, \mathbf{x}_{car})) \quad (9)$$

where

$$P_e = P_{e,must-run} + P_{e,car} - P_{PV}. \quad (10)$$

We used canonical PSO to solve for the DER schedules. The PHEV charging and the space and water heating schedules are also divided into 3 8-hour segments and are solved using co-evolutionary PSO. The simulation time is roughly the same as that when the DER are coordinated because we used the same number of particles and iterations; (4) and (5), therefore, were executed the same number of times, and the objective function is also evaluated the same number of times. Since the scheduling problem now involves several simpler problems, it is easier to generate feasible solutions and the simulation does not have to be repeated a large number of times.

We determined the value of coordination over the 3 tariff structures and 16 scenarios described in Section III-C. For brevity, we used an 8-character code to refer to a scenario: SX DX BX CX, where X is either 0 or 1. The letters S, D, B, and C refer to the solar insolation, magnitude of service demand, availability of the PHEV, and CPP status. Table IV summarizes the different meanings of X for each condition. To illustrate, scenario S1 D1 B1 C0 pertains to a sunny day, normal demand for must-run and hot water services, the PHEV is parked from 8 AM to 5 PM, and CPP is not active.

Table V shows the results of the simulations. The table shows the cost incurred when the DER are scheduled independently and when they are cooperating, and the value added by the coordination (expressed as % cost reduction). The added value is equal to the savings incurred by the end user due to the coordination.

In Tariff A (ToU energy + ToU feed-in), coordination does not bring much value to the consumers except when the demand for

TABLE V
VALUE ADDED BY COORDINATION AMONG DER

Scenario	Tariff A: ToU energy + ToU feed-in			Tariff B: ToU energy + no feed-in			Tariff C: ToU energy + ToU feed-in + peak demand charge		
	Independent (Cost, \$)	Cooperating (Cost, \$)	Added value (%)	Independent (Cost, \$)	Cooperating (Cost, \$)	Added value (%)	Independent (Cost, \$)	Cooperating (Cost, \$)	Added value (%)
S1 D1 B1 C0	3.91	3.92	-0.3	4.65	4.32	7.1	4.07	4.03	0.8
S1 D1 B0 C0	4.79	4.78	0.0	5.50	5.12	6.9	5.09	5.08	0.3
S1 D0 B1 C0	1.64	1.65	-0.6	3.02	2.31	23.5	1.72	1.64	4.3
S1 D0 B0 C0	2.51	2.51	0.0	3.43	2.86	16.8	2.65	2.63	0.5
S0 D1 B1 C0	6.01	6.00	0.2	6.04	6.02	0.2	6.15	6.12	0.4
S0 D1 B0 C0	6.88	6.88	0.0	6.88	6.89	-0.1	7.19	7.17	0.2
S0 D0 B1 C0	3.73	3.74	-0.1	4.39	3.84	12.5	3.82	3.75	1.9
S0 D0 B0 C0	4.62	4.62	0.0	4.61	4.61	0.0	4.75	4.73	0.4
S1 D1 B1 C1	7.06	7.05	0.2	8.04	7.42	7.7	7.19	7.12	1.0
S1 D1 B0 C1	14.07	14.03	0.3	15.02	14.36	4.4	14.33	14.28	0.3
S1 D0 B1 C1	2.69	1.66	38.3	4.58	2.30	49.7	2.74	1.65	39.8
S1 D0 B0 C1	5.50	5.52	-0.3	6.63	5.90	11.0	5.64	5.60	0.6
S0 D1 B1 C1	9.19	9.15	0.4	9.16	9.17	-0.1	9.27	9.21	0.6
S0 D1 B0 C1	16.12	16.10	0.1	16.15	16.12	0.2	16.42	16.42	0.0
S0 D0 B1 C1	4.85	3.74	22.8	5.36	3.89	27.4	4.84	3.76	22.3
S0 D0 B0 C1	7.67	7.61	0.8	7.62	7.60	0.2	7.73	7.68	0.7

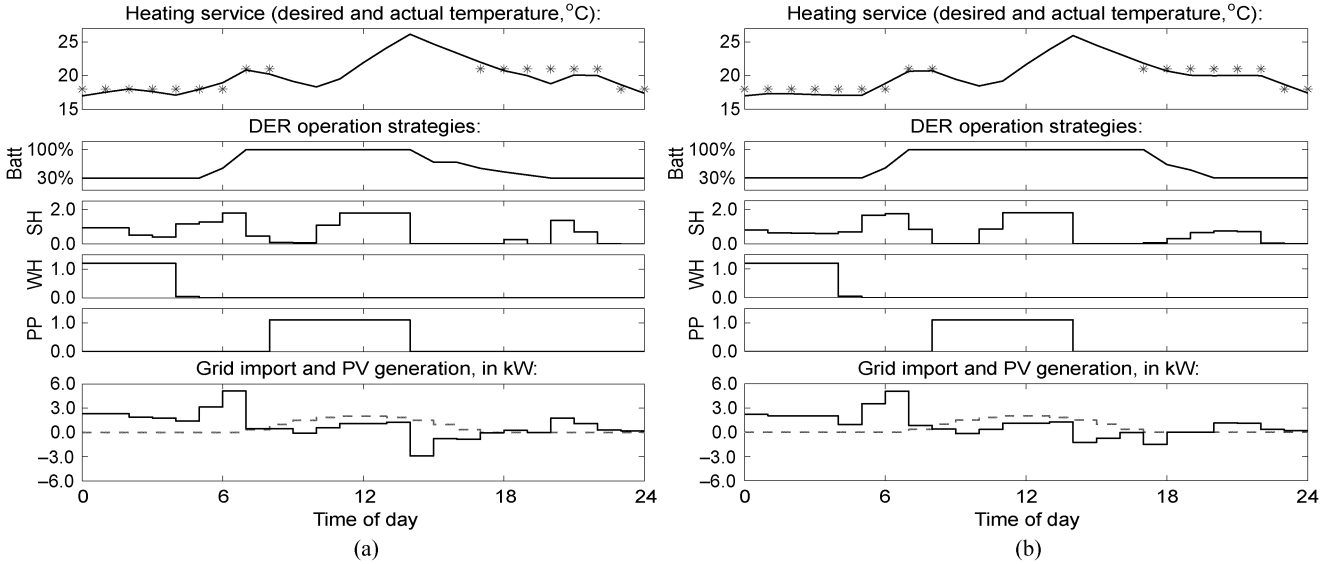


Fig. 7. DER operation schedules for scenario S1 D0 B1 C1 under Tariff A. (a) DER independent of each other. (b) DER cooperating. Shown are the state of charge of the PHEV battery (Batt), and the hourly energy consumption of the space heater (SH), water heater (WH), and pool pump (PP). Also shown are the hourly grid energy import and PV energy output (broken line).

must-run and hot water services are low, the PHEV is available and CPP is active (scenarios S1 D0 B1 C1 and S0 D0 B1 C1). The importance of coordination may be observed on Fig. 7; the figure shows the DER operation schedules for scenario S1 D0 B1 C1. When the DER are scheduled independently [Fig. 7(a)], some of the energy stored by the PHEV is discharged at the start of the peak period (2 to 3 PM), and the rest is discharged during the CPP period. The discharged energy only provides the consumption of the must-run service. The space heater is turned off from 7 to 8 PM to avoid importing energy from the grid. By 8 PM, the room becomes too cold, hence the space heating service at this hour is not provided. On the other hand, the PHEV also provides some of the space heater consumption when the DER work together [Fig. 7(b)]. Therefore, the space heating service

is provided at all hours while avoiding any energy import during the CPP period. This strategy is also apparent in scenario S0 D0 B1 C1.

Coordination among DER adds more value to the residents when feed-in compensation is not available, or Tariff B. The DER have to coordinate their operation so that the PV generation is consumed, since any exported energy receives no credit. The results show that coordination brings more value when it is sunny (S1) than when it is cloudy (S0) because of the larger amount of PV generation.

In Tariff B, coordination also brings more value when the PHEV is available and when the demand for the must-run and hot water services are low, or SX D0 B1 CX ($X = 0$ or 1). When the DER are scheduled independently in these scenarios,

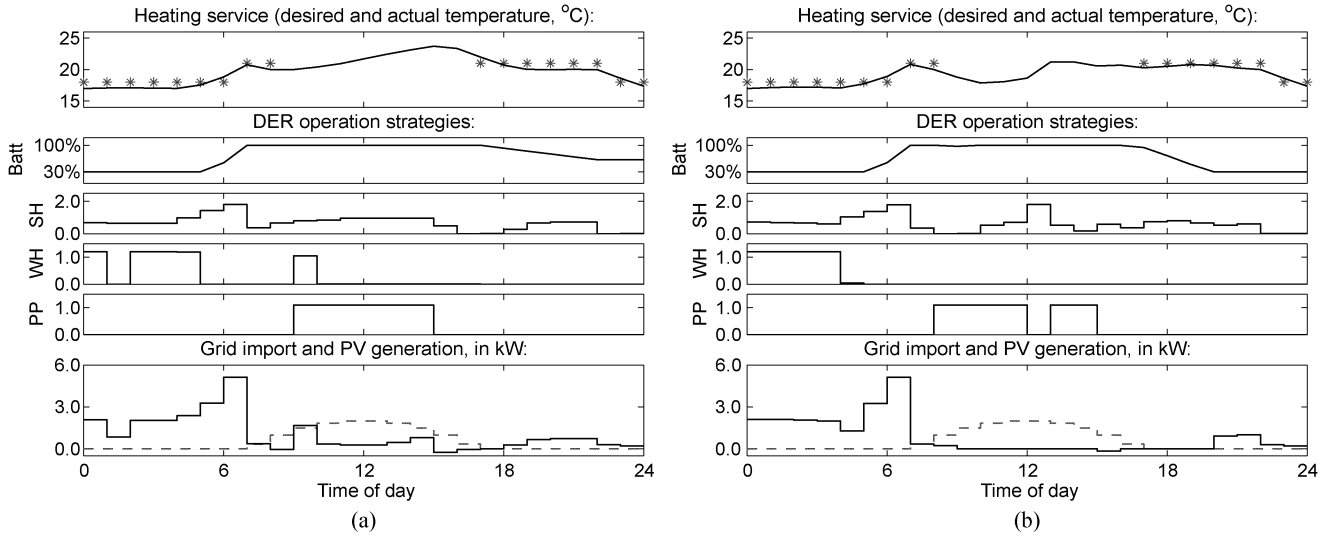


Fig. 8. DER operation schedules for scenario S1 D0 B1 C0 under Tariff B. (a) DER independent of each other. (b) DER cooperating.

the PHEV only displace the consumption of the must-run service during the evening peak and do not fully discharge. However, when the DER are cooperating, the battery fully discharges so it also provides energy to the space heater. This strategy is illustrated in Fig. 8; the figure shows the DER schedules for a sunny day, low demand, PHEV available and no CPP (S1 D0 B1 C0). The battery discharging during the CPP period also puts additional value to coordination for scenarios S1 D0 B1 C1 and S0 D0 B1 C1 because the expensive tariff during this period is avoided. Finally, the pool pump, space heater, and water heater also coordinate their operation so that energy import during the morning shoulder and peak periods are minimized.

In Tariff C where peak demand charge is levied, the value of coordination is not significant except when the service demands are low, the PHEV is available and CPP is active (scenarios S1 D0 B1 C1 and S0 D0 B1 C1), just like in Tariff A. The reasons are the same as with the other two tariffs: the PHEV fully discharge during the CPP period, hence, the expensive tariff is avoided. Furthermore, the lower service demands allows for more energy to be exported while the PHEV battery is discharging.

Coordination should add more value in Tariff C than in Tariff A because the DER should work together in order to minimize peak demand. However, the capacity charge is only applied during the peak ToU period (2–8 PM), and the capacity rate is not significant (\$0.128/kW). The added value, as shown in the table, is almost negligible.

The simulation results identify the cases where the complex scheduling problem may be decomposed into several smaller problems. The scheduling problem may be simplified if coordination does not bring any value to the end user. In the investigated cases, the scheduling may be simplified in all scenarios when under Tariff A and Tariff C except in scenarios S1 D0 B1 C1 and S0 D0 B1 C1. In Tariff B, the problem may be decomposed in a few scenarios only. There are scenarios where the value of coordination is low, and the end user may also opt to simplify the scheduling on those scenarios.

In an actual smart home, coordinated scheduling might be achieved by using a central decision-maker that controls

the operation of all the various DER. For example, this decision-support tool might reside on a computer with access to tariff arrangements and weather forecasts through the Internet, and communication to key sensors such as thermostats, a smart electricity meter with historical consumption data and the actual DER themselves. Alternatively, it would be possible and perhaps simpler to independently schedule the individual DER using the sensors, intelligence and control capabilities of the DER themselves—capabilities seen, for example, in modern reverse cycle air conditioners.

There will be inevitable tradeoffs for residential consumers between complexity, setup costs and potential savings between these two possible approaches. Much may also depend on the tariff arrangements—for example, the absence of feed-in tariff if a PV system is installed put additional value on coordinated scheduling of DER. A central coordination tool also simplifies the incorporation of some uncertainties such as, for example, the calling of CPP events by utilities.

Our proposed scheduling algorithm would seem to have some potential value in assisting consumers to assess the potential value of more complex DER and scheduling hardware, programming appropriate DER operation, and perhaps eventual incorporation into the operational scheduler itself.

In the results, there are cases where the costs are lower when the DER are independent than when cooperating. The differences are very small and we attribute this to the CPSO-R3 still not locating the optimal schedule. In these cases, coordination has no value so the decomposition of the the high-dimension optimization problem into several smaller problems simplifies the creation of the schedules.

V. CONCLUSION

The enhancements we introduced to the PSO solver were able to generate more efficient DER operation schedules for a smart home case study. The enhancements were achieved by testing several variations of coevolutionary PSO with stochastic repulsion among the particles and by choosing the best among them. The repulsion among the particles adds more randomness to the

particle trajectories at the initial iterations and it prevents premature convergence. Using the improved schedules, we determined the value of coordination among DER by comparing the results when optimal DER operation is solved in a coordinated manner versus when they are scheduled independently. There are cases where the DER can work together in order to increase net benefits (for example, to avoid export when this is not refunded, or in the presence of peak demand charge), and there are cases where coordination does not add significant value. On those cases where coordination does not add value, the complex scheduling problem may be decomposed into several simpler scheduling problems.

APPENDIX A

MODELS FOR THE SPACE HEATING AND HOT WATER SERVICES

This Appendix describes the physically based models that relate the “energy equivalents” of the space heating ($U_{ES,heat}$) and hot water ($U_{ES,water}$) services to the energy consumption of the space and water heaters ($P_{e,heat}$ and $P_{e,water}$).

The “energy equivalent” of the space heating service is the heating load $Q(t)$ of the house, and equal to the heat flowing out of the building (external air infiltration is ignored) [28]

$$Q(t) = \frac{1}{R} [\theta_{des}(t) - \theta_{out}(t)] = U_{ES,heat}(t) \quad (11)$$

$$C \frac{d\theta_{in}(t)}{dt} = P_{heat}(t) - Q(t). \quad (12)$$

R is the thermal resistance of the building shell, θ_{des} is the desired temperature, θ_{out} is the outdoor temperature (see Fig. 2), C is the heat capacity of indoor air, and P_{heat} is the heating power. The discrete time model [29] for (11) and (12) using 1-h time steps is given by

$$\theta_{in}(t+1) = \theta_{in}(t)e^{-\Delta/\tau} + RP_{heat}(t)(1 - e^{-\Delta/\tau}) + \theta_{out}(t)(1 - e^{-\Delta/\tau}), \quad (13)$$

where $\Delta = 1$ h and $\tau = RC$. The values used are $R = 18$ C°/kW, $C = 0.525$ kWh/C°, and the initial room temperature = 17°C. We assumed that the electric energy consumption of the heater is entirely converted to heat so

$$P_{e,heat}(t) = P_{heat}(t) = \mathbf{x}_{heat}. \quad (14)$$

The hot water service is provided using a storage water heater. We assumed that the water in the tank has two sections, hot and cold. The hot section is already raised to the discharge temperature and does not mix with the cold section. Cold water coming in from the bottom only mixes with the cold section.

The cold section is heated when the heater is turned on. If it takes more than 1 h to heat the entire cold section, the cold section temperature is estimated using (15), and the heating power for the entire hour is equal to the rated power of the heating coil.

If it takes less than 1 h, (16) is used to compute the heating energy for the hour, and the cold section becomes part of the hot section

$$T_{cold}(t+1) = T_{inlet} + \frac{C_0 [T_{cold}(t) - T_{inlet}] V_{cold}(t) + \eta_{coil} P_{coil} - P_{loss}}{C_0 [V_{cold}(t) + V_{inlet}(t)]}. \quad (15)$$

$$P_{e,water}(t) = \frac{C_0}{\eta_{coil}} \{ [V_{cold}(t) + V_{inlet}(t)] \Delta T - V_{cold}(t) [T_{cold}(t) - T_{inlet}] \} + P_{loss} \quad (16)$$

T_{cold} and V_{cold} are the temperature and volume of the cold section, and T_{inlet} and V_{inlet} are the inlet water temperature and volume. $P_{coil} = 1.2$ kW and $\eta_{coil} = 0.98$ are the rated power and efficiency of the heating element. $C_0 = 1.167 \times 10^{-3}$ kWh/L - C° is the specific heat of water. P_{loss} is a small amount of energy corresponding to the heat loss through the tank jacket, estimated from [30]. The inlet water should be raised by $\Delta T = 50$ C°.

The “energy equivalent” of the hot water service is the thermal energy content of the discharged water

$$U_{ES,water}(t) = C_0 \{ V_{HW}(t)(\Delta T) + V_{CW} [T_{cold}(t) - T_{inlet}] \}. \quad (17)$$

where V_{HW} is the volume discharged from the hot section and V_{CW} is the volume discharged from the cold section.

REFERENCES

- [1] L. Jiang, D.-Y. Liu, and B. Yang, “Smart home research,” in *Proc. 2004 Int. Conf. Mach. Learn. Cybern.*, Aug. 2004, vol. 2, pp. 659–663.
- [2] V. Riquebourg, D. Menga, D. Durand, B. Marhic, L. Delahoché, and C. Loge, “The smart home concept: Our immediate future,” in *Proc. 1st IEEE Int. Conf. on E-Learn. Ind. Electron.*, Dec. 2006, pp. 23–28.
- [3] C.-H. Lien, Y.-W. Bai, and M.-B. Lin, “Remote-controllable power outlet system for home power management,” *IEEE Trans. Consum. Electron.*, vol. 53, no. 4, pp. 1634–1641, Nov. 2007.
- [4] E. Sierra, A. Hossian, P. Britos, D. Rodriguez, and R. Garcia-Martinez, “Fuzzy control for improving energy management within indoor building environments,” in *Proc. Electron., Robot. Automotive Mech. Conf. 2007*, pp. 412–416.
- [5] S. Rojchaya and M. Konghirun, “Development of energy management and warning system for resident: An energy saving solution,” in *Proc. 6th Int. Conf. Electr. Eng./Electron., Comput., Telecommun. Inf. Technol.*, May 2009, vol. 1, pp. 426–429.
- [6] C.-Y. Chen, Y.-P. Tsoul, S.-C. Liao, and C.-T. Lin, “Implementing the design of smart home and achieving energy conservation,” in *Proc. 7th IEEE Int. Conf. Ind. Informatics*, Jun. 2009, pp. 273–276.
- [7] E. Williams, S. Matthews, M. Breton, and T. Brady, “Use of a computer-based system to measure and manage energy consumption in the home,” in *Proc. 2006 IEEE Int. Symp. Electron. Environment*, May 2006, pp. 167–172.
- [8] A. Roy, S. Das, and K. Basu, “A predictive framework for location-aware resource management in smart homes,” *IEEE Trans. Mobile Comput.*, vol. 6, no. 11, pp. 1270–1283, Nov. 2007.
- [9] M. C. Tu, D. Shin, D. Shin, and J. Choi, “Fundamentals and design of smart home middleware,” in *2009 Int. Joint Conf. Comput. Sci. Optimization*, Apr. 2009, vol. 1, pp. 647–650.
- [10] M. Pedrasa, E. Spooner, and I. MacGill, “Improved energy services provision through the intelligent control of distributed energy resources,” presented at the 2009 IEEE Bucharest PowerTech, Bucharest, Romania, Jun./Jul. 2009.

- [11] R. Haas, N. Nakicenovic, A. Ajanovic, T. Faber, L. Kranzl, A. Müller, and G. Resch, "Towards sustainability of energy systems: A primer on how to apply the concept of energy services to identify necessary trends and policies," *Energy Policy*, vol. 36, no. 11, pp. 4012–4021, 2008.
- [12] R. Teng and T. Yamazaki, "Bit-watt home system with hybrid power supply," in *2010 2nd Int. Conf. Comput. Automation Eng.*, Feb. 2010, vol. 5, pp. 59–63.
- [13] S. Abras, S. Pesty, S. Ploix, and M. Jacomino, "An anticipation mechanism for power management in a smart home using multi-agent systems," presented at the 3rd Int. Conf. Inf. Commun. Technol.: From Theory to Appl. 2008, Damascus, Syria, Apr. 2008.
- [14] G. Morganti, A. Perdon, G. Conte, D. Scaradozzi, and A. Brintrup, "Optimising home automation systems: A comparative study on tabu search and evolutionary algorithms," in *Proc. 17th Mediterranean Conf. Control Automation 2009*, pp. 1044–1049.
- [15] R. Negenborn, M. Houwing, B. De Schutter, and H. Hellendoorn, "Adaptive prediction model accuracy in the control of residential energy resources," in *Proc. 2008 IEEE Int. Conf. Control Applicat.*, pp. 311–316.
- [16] Energy Australia residential customer price list [Online]. Available: <http://www.energy.com.au/energy/ea.nsf/Content/NSW+Your+energy+agreement+ResidentialYA>
- [17] Energy Australia's strategic pricing study [Online]. Available: <http://www.amsi.org.au/images/electricity/pdfs/Miller.pdf>
- [18] Energy Australia business customer price list [Online]. Available: <http://www.energy.com.au/energy/ea.nsf/Content/NSW+Your+energy+agreement+BusinessYA>
- [19] M. A. Pedrasa, T. D. Spooner, and I. F. MacGill, An energy service decision-support tool for optimal energy services acquisition, Centre for Energy and Environmental Markets, Apr. 2010 [Online]. Available: <http://www.ceem.unsw.edu.au/content/userDocs/DiscussionPaper2010.pdf>, Tech. Rep.
- [20] J. Kennedy and R. Eberhart, "Particle swarm optimization," in *Proc. 1995 IEEE Int. Conf. Neural Netw.*, vol. 4, pp. 1942–1948.
- [21] J. Kennedy and R. Eberhart, "A discrete binary version of the particle swarm algorithm," in *Proc. 1997 IEEE Int. Conf. Syst., Man, Cybern.*, vol. 5, pp. 4104–4108.
- [22] F. van den Bergh and A. Engelbrecht, "A cooperative approach to particle swarm optimization," *IEEE Trans. Evol. Comput.*, vol. 8, no. 3, pp. 225–239, Jun. 2004.
- [23] J. Riget and J. Vesterstrom, A diversity-guided particle swarm optimization—The Arpso, EVALife Project Group, Dept. Comput. Sci., Univ. Aarhus, Denmark, 2002, Tech. Rep..
- [24] M. Pant, T. Radha, and V. Singh, "A simple diversity guided particle swarm optimization," in *Proc. 2007 IEEE Congr. Evol. Comput.*, pp. 3294–3299.
- [25] F. van den Bergh and A. Engelbrecht, "A study of particle swarm optimization particle trajectories," *Inf. Sci.*, vol. 176, no. 8, pp. 937–971, 2006.
- [26] M. Pedrasa, T. Spooner, and I. MacGill, "Scheduling of demand side resources using binary particle swarm optimization," *IEEE Trans. Power Syst.*, vol. 24, no. 3, pp. 1173–1181, Aug. 2009.
- [27] C. A. C. Coello, "Theoretical and numerical constraint-handling techniques used with evolutionary algorithms: A survey of the state of the art," *Comput. Methods Appl. Mech. Eng.*, vol. 191, no. 11–12, pp. 1245–1287, 2002.
- [28] H. Sauer, R. Howell, and W. Coad, *Principles of Heating, Ventilating, and Air Conditioning*. Atlanta, GA: Amer. Soc. Heating, Refrigerating and Air-Conditioning Engineers, 2001.
- [29] L. D. Ha, S. Ploix, E. Zamai, and M. Jacomino, "Tabu search for the optimization of household energy consumption," in *Proc. 2006 IEEE Int. Conf. Inf. Reuse Integr.*, pp. 86–92.
- [30] "Rheem Hot Water Manual" [Online]. Available: <http://www.rheem.com.au/manuals.asp?view=commercial>



Michael Angelo A. Pedrasa (S'07) received the B.S. and M.S. degrees in electrical engineering from the University of the Philippines, Diliman, Quezon City. He is currently working toward the Ph.D. degree at the University of New South Wales (UNSW), Sydney, Australia.

He taught at the University of the Philippines from 1997 to 2005. His studies at the UNSW are supported by the University of the Philippines and the Philippines Department of Science and Technology through the SEI-ERDT. His research interests are

power system optimization and integration of distributed energy resources to electric power systems.



Ted D. Spooner received the B.E. and M.E. degrees from the University of New South Wales, Sydney, Australia, in 1970 and 1973, respectively.

He was Project Leader for Australia's renewable energy systems testing laboratory, now known as RESLab. He has been a Senior Lecturer at the University of New South Wales in the School of Electrical Engineering and Telecommunications since 2002. His research interests are in renewable energy applications and power electronics.

Prof. Spooner is currently a Chair of Australian Standards Committee responsible for renewable energy systems. He is also the Australian representative on the International Electrotechnical Commission's (IEC) technical committee TC82 for Photovoltaics, working in the area of systems.



Iain F. MacGill received the B.E. (Elec.) degree with Honours and the M.Eng.Sci. (Biomed.) degree from the University of Melbourne, Australia, in 1987 and 1990, respectively, and the Ph.D. (Elec.) degree from the University of New South Wales, Australia, in 1999.

He is a Senior Lecturer in the School of Electrical Engineering and Telecommunications at the University of New South Wales, Sydney, Australia, and Joint Director for the university's interdisciplinary Centre for Energy and Environmental Markets. His teaching

and research interests include electricity industry restructuring and sustainable energy technologies, with a particular focus on distributed resources and energy policy.